Analytical Approach for Predicting the Thickness Distribution and Plastic Strain of an Axisymmetric Deep Drawn Part

Noor Hisham Ismail* and Mohd Nasir Tamin

Perusahaan Otomobil Nasional Sdn Bhd
40918 Shah Alam, Selangor

School of Mechanical Engineering
Faculty of Engineering
Universiti Teknologi Malaysia

hishami@proton.com

Article history

Received:
7 Nov 2019

Received in revised form:
16 Nov 2019

Accepted:
4 Dec 2019

Published online:
25 Dec 2019

*Corresponding author:
hishami@proton.com

Abstract

This contribution established an axisymmetric mathematical modeling for a prediction of induced plastic strain from sheet metal thinning of the achieved final part geometric shape in deep drawing process and the fundamentals of deformation mechanics in plane strain bending around a straight line, bending around a curve and stretch/draw forming condition. The mechanics and the closed-form solutions facilitate for the prediction of the final achieved plastic strains, stresses, and loads in the deep drawing operations without using FEM. A closed-form solution from a 2D final part geometric cross-section input was developed to calculate a deep draw effect to the achieved residual plastic strain due to variation of die profile radius, punch nose radius, sheet thickness and steel material types. Close agreement with FE results was achieved for the plastic strain values at the concave and convex interface regions with the proposed bend-unbend additional thinning method when compared to membrane calculation method.

Keywords: *Axisymmetric, Bend-Unbend, Deep Draw, Stretching, Thickness Variation.*

1. Introduction

During the early design stage of vehicle development, in order to provide a reliable prediction of structural strength, durability and NVH performance, a pre-damage of sheet metal parts formed by stamping operation need to be accounted. However, extensive human and computing resources are required to carry out the initial forming simulation for each part and panel involved in a vehicle. In addition, frequent drawing updates and part design change or improvement are inevitable along the design phase that further exhausts the resources apart from the extensive data tracking requirement for simulation model updates. In terms of detail analysis modeling, the die and punch data to be used in the forming simulation for each part in the structure is not readily available during the early stage of development. Moreover, detail forming analysis is carried out by the appointed tool maker that further imposes a constraint to the accessibility to the dies data.

Dutton et al. (1999) [1] established a method to transfer data from the forming analysis of a hydroformed frame siderail to the crashworthiness analysis (both using LSDYNA), allowing thickness, residual stress and plastic strain data selectively or

* *Corresponding authorhishami@proton.com*

incombination to be used to initialize the crash model. Based from a correlated test measurements, they have shown that the crash response is significantly affected when the effects of forming are included.

In another work, Simunovic et al. (2001) [2] assessed the influence of thickness variations and plastic strain hardening imparted in a part forming process on crash response of a vehicle. The as-formed thickness and plastic strain for front crash parts were used as input data for vehicle crash analysis. Crash modeling simulations show a moderate effect of forming on overall crash performance. However, it has been shown that for materials that have modest strain hardening, the forming effect is observable. The forming thickness variations have larger effect than the plastic hardening.

The early analytical approach for a deep drawing prediction was due to Chung and Swift (1951) [3], where the researchers formulated a theoretical treatment for a deep drawing process involving plane radial drawing where the BHF is assumed to be only concentrated at the cup rim. Woo (1964a) [4] introduced a general analytical treatment for an axisymmetric cup-drawing and hydroforming processes where plasticity theory with work-hardening material description is incorporated. Woo (1964b) [5] later formulated a numerical analysis approach by coupling the general analytical solution to examine the plastic deformation response of a conventional deep drawing process which accounts the effect of pressure, BHF, radial drawing and stretch-forming at die curvature and punch curvature zones respectively with an assumption of complete sheet-punch surface contact during the initial stage of the deep drawing progression.

Woo (1968) [6] later enhanced the previous analytical method by incorporating the effect of material anisotropy and routine in determining for the changing boundary conditions in the drawing and stretch-forming zones under different drawing stages. Taghipur and Assempour (2011) [7] analytically investigated the contributions of proportional loading to forming response of a hydro-mechanical deep drawing process. Nanu and Brabie (2012) [8] proposed an analytical model for a U stretch-bending process in predicting the effect of springback with respect to a through thickness stress distributions. A predictive model for the influence of die fillet radius to limit drawing ratio was proposed by Fazli and Arezoo (2012) [9] for a deep drawing process. Analytically, Fazlollahi et al. (2018) [10] investigated the maximum achievable limit of drawing ratio for steel/polymer sandwich material with hydro-mechanical deep drawing.

Despite the advancement of the deep drawing analytical methods, their complete analytical solution of the problems still require the use of iterative numerical technique and solver. There has been no complete closed-form solution for the simple problem of deep drawing of a cylindrical cup.

The main objective of this work is the formulation of the axisymmetric mathematical modeling for the prediction of induced plastic strain from sheet metal thinning of the achieved final part geometric shape in deep drawing process and the fundamentals of deformation mechanics in plane strain bending around a curve and stretch/draw forming condition. A closed-form solution from a 2D final part geometric cross-section input was proposed to calculate a deep draw effect to the achieved residual plastic strain due to variation of die profile radius, punch nose radius, sheet thickness and steel material types.

2. Theoretical background

The shape of the component was assumed to have already reached the final state of a single stage deep draw process where the resultant thickness distribution is induced from the maximum punch force level. The average sheet thickness under rigid-plastic condition of the plastically deformed sheet material at the side wall of the part could be approximated as:

$$t = t_0 \left(\frac{L_0}{L_{max}}\right) \quad (1)$$

where t_0, L_0 and L_{max} are the initial sheet thickness, initial cross-section length of the sheet metal blank and the cross-section arc length of the final drawn component respectively. The drawing force at the boundary of die fillet radius to the cup wall T_d is expressed as:

$$T_d = 2\pi t_d K \left[\left(\left(\frac{2}{\sqrt{3}}\right) ln\left(\frac{L_{max}}{L_0}\right)\right)^n\right]\left(R_p + t_0 + dc + r_d(1 - \sin\theta_d) - t_0 \, sin\,\theta_d\right)$$

(2)

and the drawing force at the boundary of punch nose to the cup wall T_p is:

$$T_p = 2\pi t_w K \left[\left(\left(\frac{2}{\sqrt{3}}\right) ln\left(\frac{L_{max}}{L_0}\right)\right)^n\right](R_p - r_p + (r_p + t_0)\sin\theta_p) \quad (3)$$

t_d is the sheet thickness at die fillet radius-cup wall boundary, t_w is the thickness of the cup wall, R_p is the punch radius, r_p is punch nose radius, r_d is die fillet radius, dc is the die clearance, θ_d is the wrap angle of die fillet segment and θ_p is the wrap angle of punch nose segment. K and n are the material strength coefficient and strain hardening exponent (n-value) respectively as expressed in the Hollomon hardening law, $\sigma = K(\varepsilon_p)^n$. Figure1 shows the relation of the deformed symmetrical sectional shape of the cylindrical cup and its associated tooling parameters that govern the achievement of the geometric definition of the part design intent.

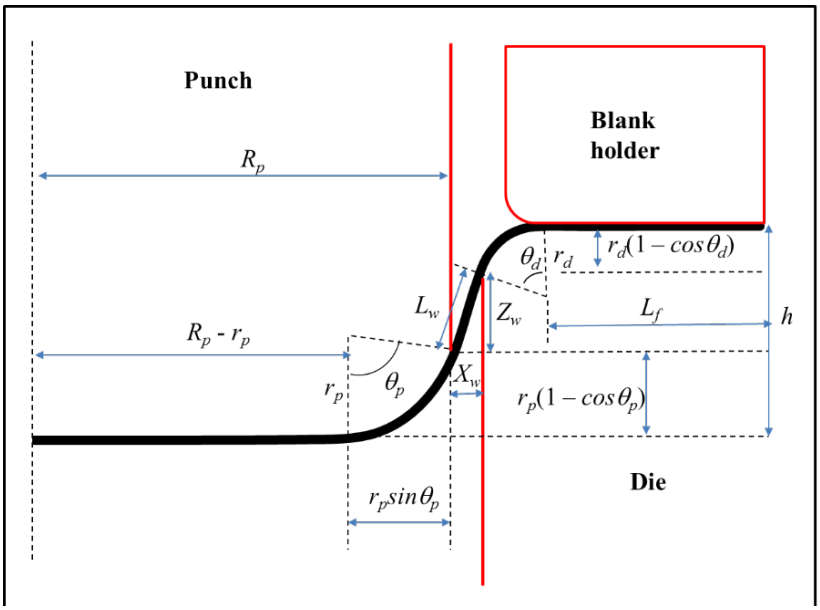

Figure 1. Symmetrical geometric description of the deformed part with respect to deep drawing tool where L_f= arc-length of the flange, L_w = arc-length of the part side wall, X_w = horizontal length of the cup wall, Z_w= vertical length of the cup wall and h = cup height

2.1. Analytical model for thickness prediction

The complex interaction between the applied forming load and plastic deformation features of a deep drawing process in relation to the deep drawing tools, friction, die clearance, part curvatures, bend-unbend, straightening, sheet thickness and material properties have been extensively examined by other researchers (Sengugupta et al., 1981; Sih et al., 1991; Huang and Chen, 1995; Moshkar and Zamanian, 1997; Jain et al., 1998; Deng et al., 1999; Siegert and Farr, 1999; Takuda et al., 1999; Delarbe and Montmitonnet, 1999; Yoshida et al., 2005; Logue et al., 2007; Morales et al., 2008; Onder and Tekkaya, 2008; Deng et al., 2009; Levy et al., 2009; Raghavan et al., 2010; Anil Kumar et al., 2010; Hudgins et al., 2010; Arezodar and Eghbali, 2012; He at al., 2013; Marty-Delgado, 2013; Qin et al., 2015; Gurun and Karaagac, 2015; Simoes et al., 2017; Martinez et al., 2017; Wang et al., 2017; López and and Regueras, 2017; Kalkan et al., 2017; Hattalli and Srivatsa, 2018; Kong et al, 2018) [11-40].

Relation (1) to (3) were further expanded to address the various responses of the sheet material due to the moving boundary conditions particularly at the die fillet segment and punch nose region. Results of the derived equations for thickness prediction at various cylindrical cup segments were arranged in Table 1.

Table 1. Predicted thickness at various segments of the cup under different deep drawing conditions and various interactive factors.

No.	Assumptions of the drawing conditions and factors combination	Predicted thickness, mm
1	Deep draw conditions that facilitate a successful final part deformation where *UTS* and *n*-value affect the material hardening response to the plastic deformation. 1. Low stretching severity, $t_0/r_d \leq 0.2$	$t_d = \frac{t_0 UTS}{K\left[\left(\left(\frac{2}{\sqrt{3}}\right) ln\left(\frac{L_{max}}{L_0}\right)\right)^n\right]}$ (4)

	2. Low bending severity, $r_d/t_0 \geq 5$ 3. Typical mild steel and HSLA with $t_0 \leq 0.7$ and $UTS \leq 400$ MPa 4. Higher strength steel with $t_0 \geq 0.7$ mm and $UTS \geq 400$ MPa	A change of deep drawn variables at the surface of the tool curvature could be assumed to follow an exponential form due to the geometric constraint imposed to the drawn material. $L0$ and L_{max} are the initial sheet thickness, initial cross-section length of the sheet metal blank and the cross-section arc length of the final drawn component respectively.
2	A situation where resistance to the localized thinning is low at the curvature of die corner radius. Thinning is therefore expressed as: 1. Large stretching and thus thinning severity, $t_0/r_d > 0.2$ 2. Large bending and unbending severity, $r_d/t_0 < 5$ 3. Typical mild steel and HSS with $t_0 \leq 0.7$ mm, $UTS \leq 400$ MPa 4. Thickness change as a result of friction at die profile radius	$t_d = \frac{t_0 UTS}{K\left[\left(\left(\frac{2}{\sqrt{3}}\right) ln\left(\frac{L_{max}}{L_0}\right)\right)^n\right]} e^{(-\mu_d \theta_d)}$ (5a) The sheet thickness at an arc length fraction of $0 \leq f \leq 1$ was assumed to change exponentially with both the achieved thickness strain of the boundary of the cup wall and wrap angle. Therefore, the overall sheet thickness at the curvature of the drawn part could be expressed as $t = t_0 exp\left[\ln\left(\frac{t_d}{t_0}\right) e^{-f\theta_d}\right]$ (5b) $f = 0$ is an arc length fraction at the boundary of die profile radius to cup wall. Sheet thickness at the boundary of die profile radius to the flange ($f = 1$) is therefore $t = t_0 exp\left[\ln\left(\frac{t_d}{t_0}\right) e^{-\theta_d}\right]$ (5c)
3	The change in the average sheet thickness at the cup wall segment was determined by equating (2) and (3) and solved for t_w. Assumption: equal tensile load level of the cup wall which is stretched between both boundaries of die profile region-cup wall and punch nose-cup wall.	$t_w = \left[t_d\left(R_p + t_0 + dc + r_d(1 - sin\,\theta_d) - t_0\, sin\,\theta_d\right)\right] / [(R_p - r_p + (r_p + t_0)\sin\theta_p)]$ (6a) The side wall thickness t_w could be assumed to change linearly throughout the arc length of the side wall as $t_w = t_p + f\left(t_d - t_p\right)$ (6b) where $0 \leq f \leq 1$ is the fraction of the side wall length. $f = 0$ is the side wall fraction at the boundary of the punch corner radius to the side wall while $f = 1$ is the side wall fraction at the boundary of the die corner radius to the side wall.
4	General deep drawing conditions at the punch corner radius with large influence of stretching and thinning ($t/t_0 < 0.7$) under bend-unbend and straightening of the sheet once leaving the punch corner radius towards the side wall unsupported region. Additional sheet thinning at the boundary of punch corner radius to the side wall is contributed by: 1. Minimal localized thinning influence at die corner radius with $t_0/r_d < 0.33$ (lower bending severity of $r_d/t_0 > 3$). 2. Strong stretching severity and thus thinning of $t_0/r_p \leq 0.1$ at punch corner radius (strong bending severity of $r_p/t_0 \geq 10$) 3. Blank thickness of $t_0 \leq 1$ mm. 4. Plane strain deformation of the side wall. 5. Typical mild steel and HSLA steel with $UTS < 600$ MPa.	$t_p = \frac{t_0 UTS}{K\left[\left(\left(\frac{2}{\sqrt{3}}\right) ln\left(\frac{L_{max}}{L_0}\right)\right)^n\right]} e^{(-\mu_p \theta_p)}$ (7) Similar as in the case of die fillet radius, the change of deep drawn variables at the surface of the punch profile radius, which is in contact with the tool curvature, could be assumed to follow an exponential form due to the geometric constraint imposed to the drawn material.
5	Typical sheet metal stretching level of $t/t_0 > 0.7$ at the boundary of the punch corner radius to the side wall due to: 1. Tensile tearing driven failure mechanism at punch nose area, $t_0/r_p > 0.1$ (bending with tearing prone severity of $r_p/t_0 < 10$) 2. Blank thickness of $t_0 \leq 1$ mm 3. Typical mild steel and HSLA steel blank sheet material with $UTS < 600$ MPa	By volume constancy principle, the sheet thickness at the boundary of punch nose-cup wall could be described as $t_p = \sqrt{\left[r_p^2 + t_w(2r_p + t_w)\frac{\theta_p}{\theta r}\right]} - r_p$ (8a) Where θ' is a change of the punch wrap angle due to the additional stretching of the sheet metal from the straightening of the wall angle $\theta_w = \min(\theta_d, \theta_p)$

		$\theta' = \theta_p + \lvert\theta_p - \theta_w\rvert$ (8b)
6	Thinning at the boundary of punch corner radius to side wall is not strong (stretching level of $t/t_0 \geq 0.8$). Insignificant change in wall thickness due to: 1. Equal tensile load level of the cup wall between both boundaries of die profile region-cup wall and punch nose-cup wall 2. Strong stretching severity of $t_0/r_d > 0.33$ at die corner radius (strong bending severity of $r_d/t_0 < 3$) at die profile region. 3. Thickness of sheet metal of $t_0 > 1$ mm which facilitates draw-in. 4. AHSS blank sheet material with $UTS > 600$ MPa which could fracture at die corner area or enhance the draw-in.	$t_p = \sqrt{\left[r_p^2 + t_0\left(\frac{L_0}{L_{max}}\right)(2r_p + t_0\left(\frac{L_0}{L_{max}}\right))\frac{\theta_p}{\theta'}\right]} - r_p$ (9a) From (7) to (9), the sheet thickness at the boundary of punch nose to the cup bottom ($f = 1$) is $t = t_0 exp\left[\ln\left(\frac{t_p}{t_0}\right)e^{-\theta_p}\right]$ (9b) The sheet thickness at the center of the cylindrical cup is assumed to be equal to the sheet thickness at the boundary of the punch nose to the cup bottom as in (9a).

2.2. Straining of the deep drawn cylindrical cup

Once the achieved thicknesses at the geometric entities of the cylindrical cup are known, the straining level of the part could be determined. For part geometry with a curvature, the longitudinal principal strain at the outer sheet layer or convex side is

$$\varepsilon_{1o} = \ln\frac{(2t_0/t)(r+t)}{(2r+t)} \quad (10)$$

At the inner sheet layer or concave side of the bend material, when stretching is mild ($t/t_0 \geq 0.7$), the longitudinal strain is expressed as

$$\varepsilon_{1i} = \ln\frac{(2t_0/t)(r+t)}{(2r+t)} - \ln\left[1 + \frac{t}{2r}\right] = \ln\frac{(4rt_0/t)(r+t)}{(2r+t)^2} \quad (11)$$

However, under stronger sheet stretching condition ($t/t_0 < 0.7$),

$$\varepsilon_{1i} = \ln\frac{(2t_0/t)(r)}{(2r+t)} - \ln\left[1 + \frac{t}{2r}\right] = \ln\frac{4t_0}{t}\left(\frac{r}{2r+t}\right)^2 \quad (12)$$

To account for the variation of through thickness straining due to bending and stretching, curvature correction to the membrane thickness strain expression at the convex side of the sheet due to thinning from the stretched outer sheet layer is required. Therefore

$$\varepsilon_{3o} = \ln\frac{t}{t_0} + \ln\frac{r+t}{r+t_0} = \ln\left(\frac{t}{t_0}\frac{r+t}{r+t_0}\right) \quad (13)$$

Similarly, at the concave side, thickening due to surface compression at the inner sheet layer could be expressed as

$$\varepsilon_{3i} = \ln\frac{t}{t_0} - \ln\frac{r+t}{r+t_0} = \ln\left(\frac{t}{t_0}\frac{r+t_0}{r+t}\right) \quad (14)$$

By conservation of volume, the circumferential strain is

$$\varepsilon_2 = -(\varepsilon_1 + \varepsilon_3) \quad (15)$$

Finally, with strain path of $\alpha = \frac{\varepsilon_2}{\varepsilon_1}$, the equivalent plastic strain is therefore

$$\varepsilon_p = \varepsilon_1\left(\frac{2}{\sqrt{3}}\right)\sqrt{1 + \alpha + \alpha^2} \quad (16)$$

3. Methodology

3.1. Tensile test

The work started with the uniaxial tensile test of low carbon mild steel (SPCC) in order to obtain the basic tensile material properties at different strain rates. Curve fitting was performed for the description of its hardening plastic flow law as input for the cylindrical deep draw FE simulation.

3.2. Cup drawing experiment

Next, a cup drawing experimental works was conducted under slow loading condition to investigate the material response when subjected to sheet metal forming conditions. The blank was initially a circular sheet of 85 mm diameter with a thickness of 0.7 mm. Figure 2 illustrates the dimensional configuration of the analysis.

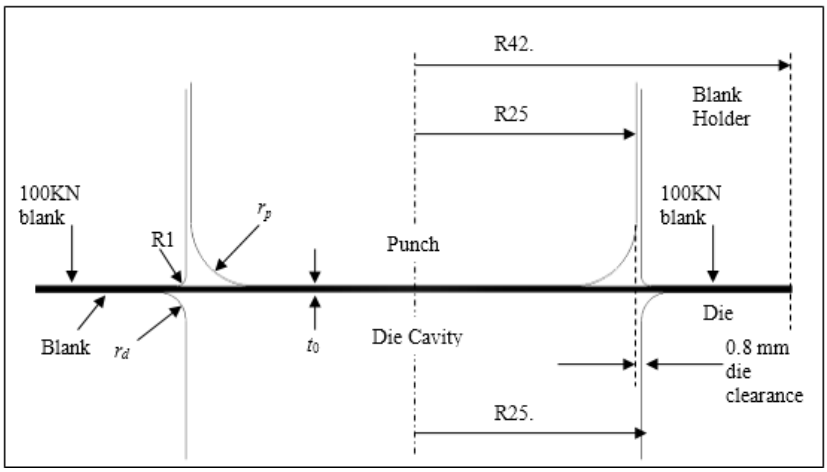

Figure 2. Schematic of the main initial dimension for the cup draw configuration.

3.3. Finite element simulation

Correlation studies of the drawn cup with FE simulation methods were performed using Abaqus/Standard simulation software to determine the friction coefficients that were not readily measured by the physical test approach. The geometry, load, materials and other details for the FE model were based from the configuration of the experimental conditions of the deep drawn cylindrical cup. To minimize potential error contributed by the mesh quality, the mesh of the blank was discretized into several segments to account for the severity of different deformation response at several different local areas during the computational process. The blank sheet metal was treated as deformable and meshed with reduced integration C3D8R solid type element. The mechanical interactions between the contact surfaces of sheet-tools were accounted using a Coulomb contact friction law. Validation of the FEA model was performed by examining the obtained experimental punch force value against the simulated force. Finite element implicit code was used to avoid parameters that could also result in unrealistic inertial effects.

3.4. Analytical model vs FE

The analytical model was validated by evaluating the results from both the analytical model calculation and FE simulation outputs. FE results at the maximum punch force state was selected for the evaluation since it represented the near end state of the deep drawing process in which the component had reached a condition where its shape had complied with the intended design configuration. Several FE results with variations in die corner radius (2 mm to 8 mm), punch corner radius (2 mm to 10 mm) and sheet thickness (0.7 mm to 2.0 mm) while maintaining the sheet material with SPCC were applied for the evaluation of the analytical model. The influence of steel material grades (ranging from mild steel, HSLA and AHSS) to the straining of the drawn part was also examined against the result from the analytical model. Figure 4 is the true stress-true strain curves of all the steel grades applied in the analytical model.

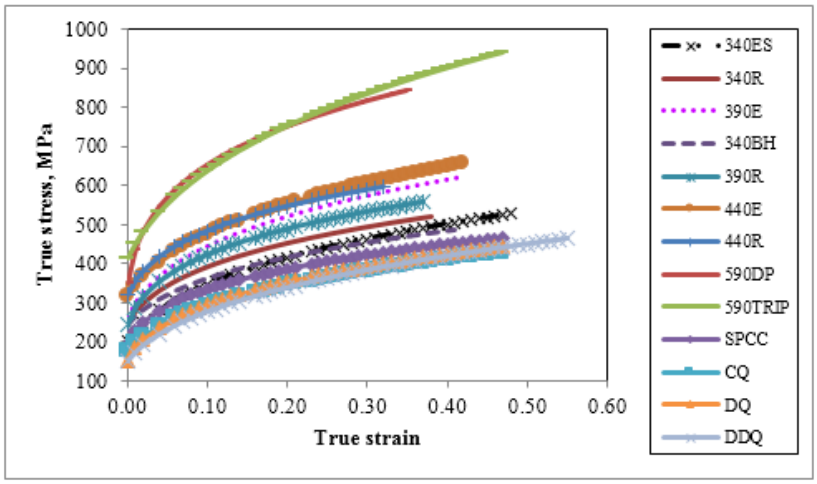

Figure 3. True stress-true strain curves of the steel grades for the verification of the analytical model.

4. Result and discussion

4.1. Experimental and FE correlation of cup drawing process

This segment presented the correlation results of an experimental cup drawing process of a 0.7 mm thick SPCC mild steel sheet metal using a numerical simulation approach. The objective of the simulation was to identify the relevant parameters of the SPCC blank material in the cup drawing process. The values of the identified parameters would be extended into the detail FE analysis for the verification of the analytical model. Coefficient of friction with a value of 0.08 for the die contact surface together with stabilization parameter of 0.01 for the contact controls produced closer agreement for the punch force-punch displacement profile with the experimental result as indicated in the insert (Figure 4).

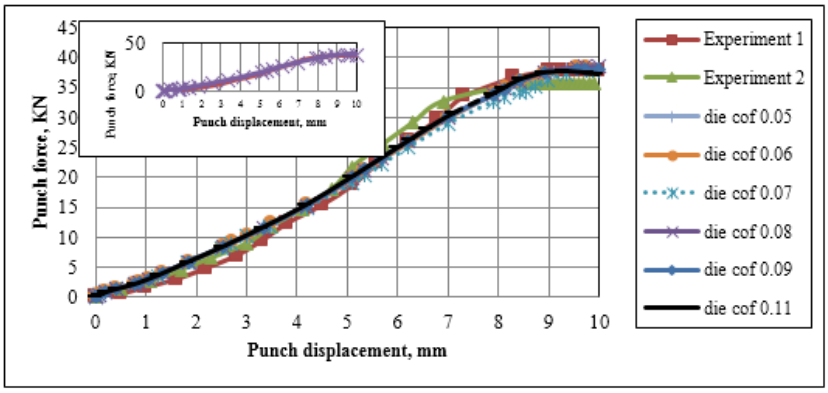

Figure 4. Punch force vs punch displacement (correlation for coefficient of friction at die)

Coefficient of friction with a value of 0.20 and 0.08 for the punch and die contact surface respectively, together with stabilization parameter of 0.01 for the contact controls produced closer agreement for the punch force-punch displacement profile with the experimental result (Figure 5).

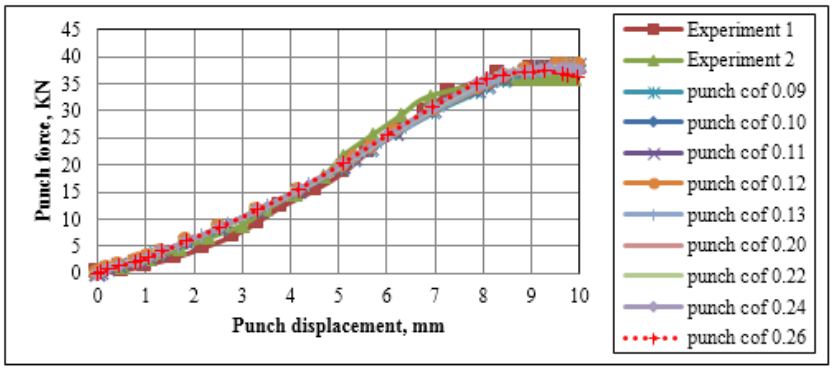

Figure 5. Punch force vs punch displacement (correlation for coefficient of friction at punch)

Coefficient of friction with a value of 0.11, 0.20 and 0.08 for the blank holder, punch and die contact surface respectively, together with stabilization parameter of 0.01 for the contact controls produced closer agreement for the punch force-punch displacement profile with the experimental result (Figure 6). In addition, element layers with odd numbers produced closer agreement for the punch force-punch displacement profile with the experimental result (Figure 7).

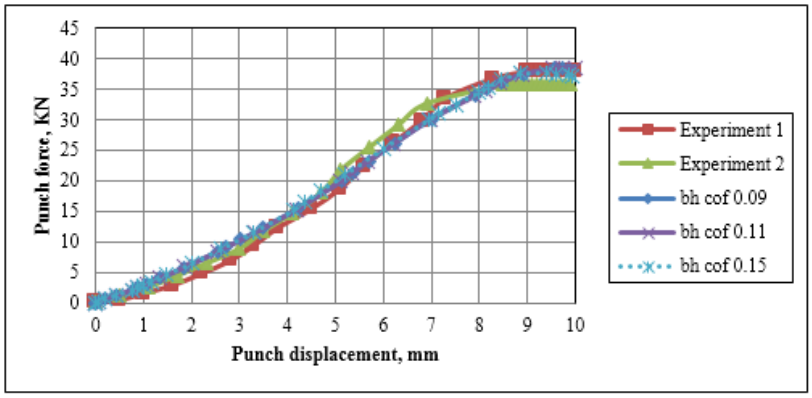

Figure 6. Punch force vs punch displacement (correlation for coefficient of friction at blank holder)

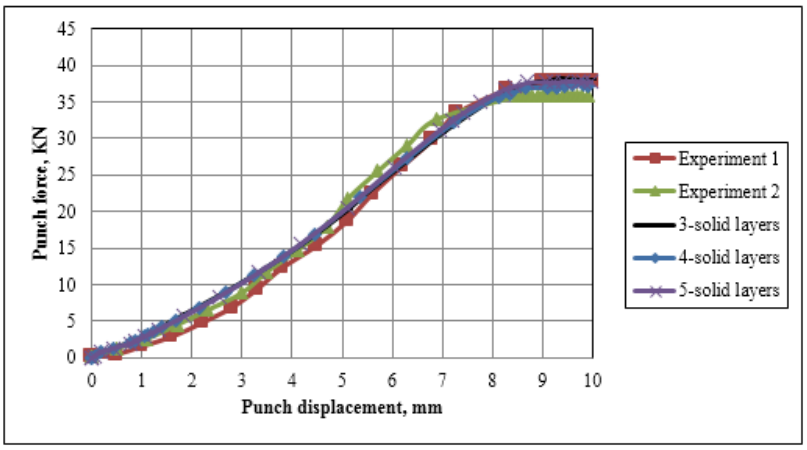

Figure 7. Punch force vs punch displacement (correlation for layers of solid element through the blank thickness)

In the correlated model, the coefficient of friction values of 0.2 were used for the interfaces between the blank and the punch, 0.08 for the blank and die and 0.11 for the blank and the blank holder. These friction coefficient values were in good agreement with Darendeliler et al. (2002) [41] findings and optimum in the present FE simulation. Some experimental-numerical discrepancies appeared at higher level of punch displacement. They were attributed to the effect, not captured by the FE model such as micro-crack formation that occurs before the point of maximum load.

4.2. Validation of the analytical model with FEA result

4.2.1 Thickness prediction result

Figure 8 shows the comparison of thickness distribution results between the analytical model and FEA for SPCC material with r_d =3 mm, r_p =7 mm and t_0 =0.7 mm. Good agreement was shown between the two results except at the cup center, cup rim positions and punch corner radius-wall boundary region. Nevertheless, a conservative prediction of thickness value was shown for these locations.

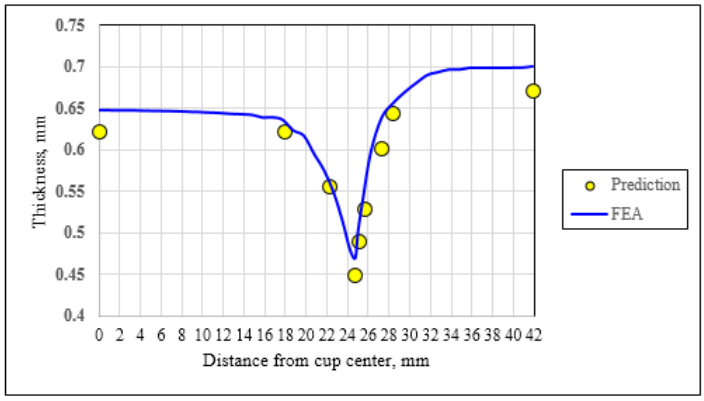

Figure 8. FEA vs Prediction: thickness distribution (SPCC, r_d = 3 mm, r_p = 7 mm, t_0 = 0.7 mm)

The overall comparison of the FEA and analytical prediction on thickness results for several different locations within the cylindrical cup were indicated in Figure 9 and Figure 10. Results for all die radius, punch corner radius, sheet thickness and steel material grade variations in this research were summarized inside those figures. The thickness prediction from the analytical model was in a very close agreement with the FEA simulation results.

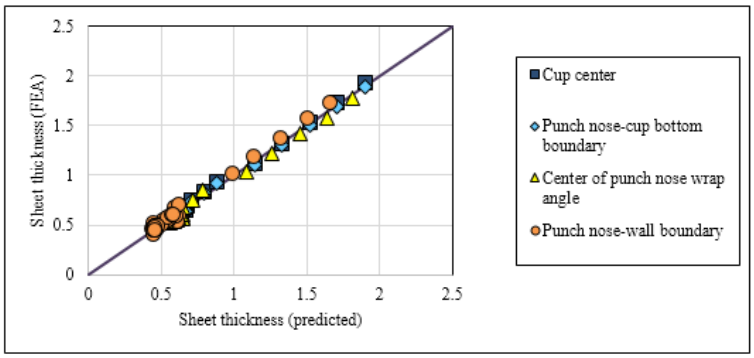

Figure 9. FEA vs Prediction: thickness distribution at locations from cup center to punch nose-side wall boundary (with variations of die radius, punch radius, thickness and steel material grades).

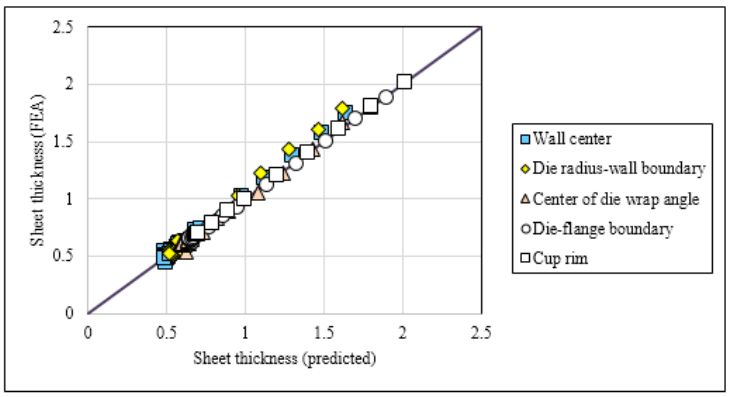

Figure 10. FEA vs Prediction: thickness distribution at locations from center of cup wall to the cup rim (with variations of die radius, punch radius, thickness and steel material grades).

4.2.2 Strain prediction result

Figure 11 to Figure 14 show the comparison of the principal strains and equivalent plastic strain distribution results between the analytical model and FEA for SPCC material with r_d =3 mm, r_p =7 mm and t_0 =0.7 mm. Good agreement was shown between the two results except at the cup center, cup rim positions and punch corner radius-wall boundary region. Nevertheless, a conservative prediction of strain value was shown for these locations. The value of the predicted circumferential strain at the cup inner surface or the convex side of the die edge radius was very compressive compared to the FEA results. However, their values were very small to significantly affect the overall results of the equivalent plastic strain.

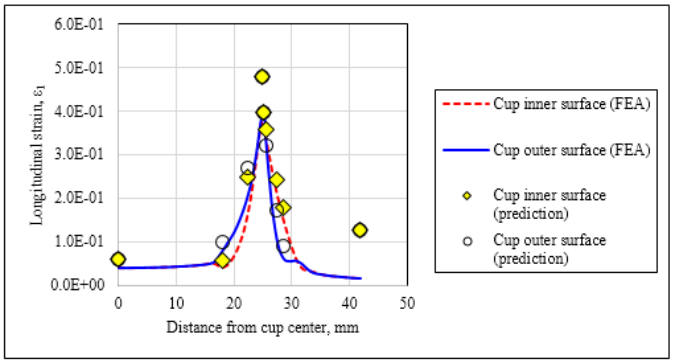

Figure 11. FEA vs Prediction: Longitudinal principal strain (SPCC, r_d = 3 mm, r_p = 7 mm, t_0 = 0.7 mm)

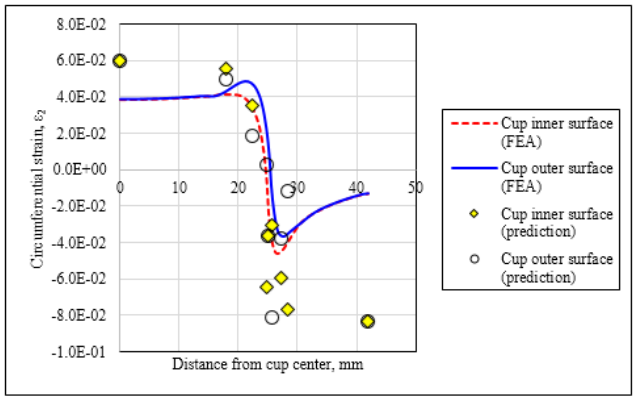

Figure 12. FEA vs Prediction: Circumferential principal strain (SPCC, r_d = 3 mm, r_p = 7 mm, t_0 = 0.7 mm)

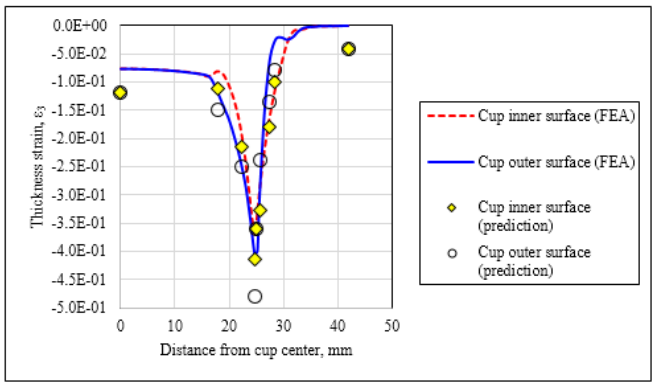

Figure 13. FEA vs Prediction: Thickness principal strain (SPCC, r_d = 3 mm, r_p = 7 mm, t_0 = 0.7 mm)

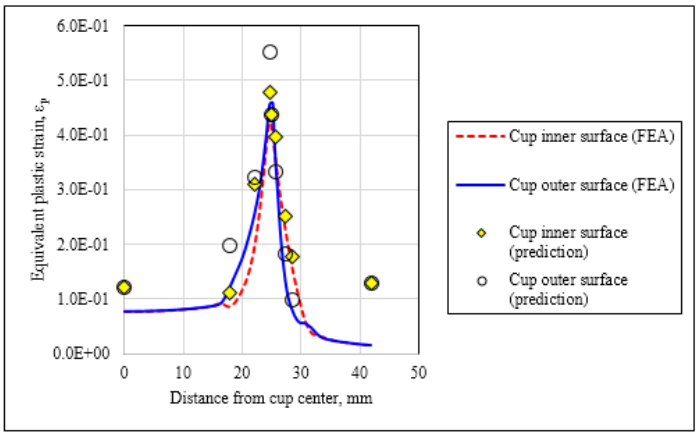

Figure 14. FEA vs Prediction: Equivalent plastic strain (SPCC, r_d = 3 mm, r_p = 7 mm, t_0 = 0.7 mm)

In general, the equivalent plastic strain prediction using the analytical model could be concluded as conservative particularly at the cup rim, boundary of die edge radius to the cup wall, center of the cup wall, boundary of the punch edge radius to the cup wall, center of punch edge radius, boundary of punch edge radius to cup bottom and cup center.

5. Conclusion

The analytical model for the prediction of thickness distribution and residual strain induced by an axisymmetric deep draw operation was proposed and validated using a correlated FE simulation model. Good agreement of results was achieved. A mapping function of the induced plastic strain with respect to part's geometrical attributes in incorporating the manufacturing load history effect for the next stage of numerical simulation was formulated. The model for bending severity under tension loading at die profile radius and punch nose was proposed where the straining effect from the interaction of punch and die wrap angles with sheet initial thickness and material property was determined for a stretch/draw condition.

Acknowledgement

The authors would like to acknowledge all CAE team, Production Engineering and Material Lab members from Miyazu Malaysia Sdn Bhd and Perusahaan Otomobil Nasional Sdn Bhd who have contributed their professional efforts, talents, and personal support to this work.

6. References

[1] Dutton, T., Iregbu, S., Sturt, R., Kellicut, A., Cowell, B. and Kavikondala, K., "The Effect of Forming on the Crashworthiness of Vehicles with Hydroformed Frame Siderails", International Body Engineering Conference and Exposition, Detroit, Michigan, September 28–30, 1999, SAE Paper 1999-01-3208.
[2] Simunovic, S., Shaw, J. and Aramayo, G.A., "Steel Processing Effects on Impact Deformation of UltraLight Steel Auto Body", Proceedings of SAE 2001 World Congress, Detroit, Michigan (2001), Paper no. 2001-01-1056.
[3] Chung, S.Y. and Swift, H.W., "Cup-drawing from a Flat Blank: Part I. Experimental Investigation", Proceedings of the Institution of Mechanical Engineers, Vol 165, (1951), pp 199-211.
[4] Woo, D.M., "Analysis of the Cup-Drawing Process", J. Mech. Engng. Sci. Vol 6, No 2, (1964a), pp 116-131.
[5] Woo, D.M., "The Analysis of Axisymmetric Forming of Sheet Metal and the Hydrostatic Bulging Process", Int. J. Mech. Sci., Vol 6, (1964b), pp 303-317.
[6] Woo, D.M., "On the Complete Solution of the Deep-Drawing Problem", Int. J. Mech. Sci., Vol 10, (1968), pp 83-94.
[7] Taghipur, E. and Assempour, A., "The Effects of Proportional Loading, Plane Stress, and Constant Thickness Assumptions on Hydro-Mechanical Deep Drawing Process", International Journal of Mechanical Sciences, Vol 53 (2011), pp329-337.
[8] Nanu, N. and Brabie, G., "Analytical Model for Prediction of Springback Parameters in the case of a U Stretch-Bending Process as a Function of Stresses Distribution in the Sheet Thickness", International Journal of Mechanical Sciences, Vol 64, (2011), pp 11-21.
[9] Fazli, A. and Arezoo, B., "Prediction of Limiting Drawing Ratio Considering the Effective Parameters of Die Arc Region", Journal of Materials Processing Technology, Vol 212, (2012), pp 745-751.
[10] Fazlollahi, M., Morovvati, M. R. and Mollaei Dariani, B., "Theoretical, numerical and experimental investigation of hydro-mechanical deep drawing of steel/polymer/steel sandwich sheets", Proceedings of the Institution of Mechanical Engineers, Part B: Journal of Engineering Manufacture, 095440541878017. (2018).
[11] Sengupta, A.K., Foog, B. and Ghosh, S.K., "On the Mechanism behind the Punch-Blank Surface Conformation in Stretch Forming and Deep Drawing", Journal of Mechanical Working Technology, Vol 5, (1981), pp 181-210.
[12] Sih, G.C., Chao, C.K., Liu, C.H., and Lin, S.Y., "Deep Drawing of Plastically and Incrementally Deformed Circular Cylindrical Cup", Theoretical and Applied Fracture Mechanics, Vol 15, (1991), pp 35-61.
[13] Huang, Y.M. and Chen, J.W., "Influence of Die Arc on Formability in Cylindrical Cup-Drawing", Journal of Materials Processing Technology, Vol 55, (1995), pp 360-369.
[14] Moshkar, M.M. and Zamanian, A., "Optimization of the Tool Geometry in the Deep Drawing of Aluminum", Journal of Materials Processing Technology, Vol 72, (1997), pp 363-370.
[15] Jain, M., Allin, J. and Bull, M.J., "Deep Drawing Characteristics of Automotive Aluminum Alloys", Materials Science and Engineering A256, (1998), pp 69-82.
[16] Deng, Z., Bleck, W., Lovell, M.R. and Papamantellos, K., "A General Approach for Predicting the Drawing Fracture Load and Limit Drawing Ratio of an Axisymmetric Drawing Process", Metallurgical and Materials Transaction A, Vol 30A, (1999), pp 2619-2627.
[17] Siegert, K. and Farr, M., "Optimized Radii for Draw Dies", International Congress and Exposition, Detroit, Michigan, March 1-4, 1999. SAE Paper 1999-01-0685.
[18] Takuda, H., Mori, K. and Hatta, N., "The Application of Some Criteria for Ductile Fracture to the Prediction of the Forming Limit of Sheet Metals", Journal of Materials Processing Technology, Vol 95, (1999), pp 116-121.
[19] Delarbe, D. and Montmitonnet, P., "Experimental and Numerical Study of the Ironing of Stainless Steel Cups", Journal of Materials Processing Technology, Vol 91, (1999), pp 95-104.
[20] Yoshida, M., Yoshida, F., Konishi, H. and Fukumoto, K., "Fracture Limits of Sheet Metals under Stretch Bending", Int. J. Mech. Sci., Vol 47, No 12, (2005), pp 1885-1896.
[21] Logue, B., Dingle, M. and Duncan, J.L., "Side-Wall Thickness in Draw Die Forming", Journal of Materials Processing Technology, Vol 182, (2007), pp 191-194.
[22] Morales, D., Vallellano, C. and Garcia-Lomas, F.J., "Strain Gradient Effect in the Failurte of Stretch-Bend Metal Sheets", 12th International Research/Expert Conference, "Trends in the Development of Machinery and Associated Technology", TMT 2008, Istanbul, Turkey, 26-30 August, 2008.
[23] Onder, E. and Tekkaya, A.E., "Numerical Simulation of Various Cross Sectional Workpieces Using Conventional Deep Drawing and Hydroforming Technologies", International Journal of Machine Tools and Manufacture, Vol 48, (2008), pp 532-542.
[24] Deng, Y.C., Chen, G., Yang, X.F. and Xu, T., "Strain Limit Dependence on Stress Triaxiality for Pressure Vessel Steel", Journal of Physics: Conference Series, (2009). doi:10.1088/1742-6596/181/1/012071.
[25] Levy, B.S. and Van Tyne, C.J., "Predicting Breakage on a Die Radius with a Straight Bend Axis during Sheet Forming", Journal of Materials Processing Technology, Vol 209, (2009), pp 2038-2046.
[26] Raghavan, K.S. and Garrison Jr, W.M., "An Investigation of the Relative Effects of Thickness and Strength on the Formability of Steel Sheet", Materials Science and Engineering A, Vol 527, (2010), pp 5565-5574.
[27] Anil Kumar, A., Satapathy, S. and Ravi Kumar, D., "Effect of Shet Thickness and Punch Roughness on Formability of Sheets in Hydromechanical Deep Drawing", Journal of Materials Engineering and Performance, Vol 19, (2010), pp 1150-1160.
[28] Hudgins, A.W., Matlock, D.K., Speer, J.G. and Van Tyne, C.J., "Predicting Instability at Die Radii in Advanced High

Strength Steels', Journal of Materials Processing Technology, Vol 210, (2010), pp 741-750.
[29] Arezodar, A.F. and Eghbali, A., "Evaluating the Parameters Affecting the Distribution of Thickness in Cup Deep Drawing of ST14 Sheet", Journal of Advanced Science and Engineering Research,Vol 2, (2012), pp 223-231.
[30] He, J., Xia, Z.C., Zeng, D. and Li, S., "Forming Limits of a Sheet Metal After Continuous-Bending-Under-Tension Loading", Journal of Engineering Materials and Technology, Vol 135, (2013), 031009-1 – 031009-8.
[31] Marty-Delgado, J.R., Batalha, G.F., Bernal-Aguilar, Y. and Ramos-Diaz, M., "Control of Optimum Parameters in Cylindrical Deep Drawing of Sheet Metal Using Genetic Algorithm and Finite Element Methods", 7th Brazilian Congress on Manufacturing Engineering, May 20th-24th, 2013, Penedo, Italiaia, RJ Brazil.
[32] Qin, S.J., Gai, B.B., Kong, X.H. and Deng, C., "Analytical Solutions of Strain of Axisymmetric Curved Part in Sheet Metal Forming Process using Direct Integral Method", International Journal of Mechanical Sciences, Vol 101-102, (2015), pp 49-58.
[33] Gurun, H. and Karaagac, I., "The Experimental Investigation of Effects of Multiple Parameters on the Formability of DC01 Sheet Metal", Journal of Mechanical Engineering, Vol 61, No 11, (2015), pp 651-662.
[34] Simões, V. M., Oliveira, M. C., Neto, D. M., Cunha, P. M., Laurent, H., Alves, J. L. and Menezes, L. F., "Numerical study of springback using the split-ring test: influence of the clearance between the die and the punch", International Journal of Material Forming, Vol 11, No 2, (2017), pp 325–337.
[35] Martínez, A., Miguel, V. and Coello, J., "A new approach to evaluate bending forces for deep-drawing operations of a TRIP700 +EBT steel sheet", International Journal of Material Forming, Vol 11, No 5, (2017), pp 619–641.
[36] Wang, C., Ma, R., Zhao, J. and Zhao, J., "Calculation method and experimental study of coulomb friction coefficient in sheet metal forming", Journal of Manufacturing Processes, Vol 27, (2017), pp 126–137.
[37] López, A. M. C. and Regueras, J. M. G., "Formability of dual-phase steels in deep drawing of rectangular parts: Influence of blank thickness and die radius", AIP Conference Proceedings 1896, 020026 (2017). doi:10.1063/1.5007983
[38] Kalkan, H., Hacaloglu, T. and Kaftanoglu, B., "Experimental investigation of friction in deep drawing", The International Journal of Advanced Manufacturing Technology, Vol 92, No 9-12, (2017), pp 3311-3318.
[39] Hattalli, V. L., and Srivatsa, S. R., "Sheet Metal Forming Processes – Recent Technological Advances", Materials Today: Proceedings, Vol 5, No 1, (2018), pp 2564–2574.
[40] Kong, Z., Zhang, J., Li, H., and Kong, N., "Deep drawing and bulging forming limit of dual-phase steel under different mechanical properties", The International Journal of Advanced Manufacturing Technology, Vol 97, No 5-8, (2018), pp 2111–2124.
[41] Darendeliler, H., Akkok, M. and Yucesoy, C.A,."Effect of Variable Friction Coefficient on Sheet Metal Drawing", Tribology International, 35, (2002), pp 97-104.